Research Article | Vol. 7, No. 9 | 1 Sep 2017 | OPTICAL MATERIALS EXPRESS 3377

Optical Materials EXPRESS

Laser testing of anti-reflection micro-structures fabricated in ZnSe and chromium-ion doped ZnSe laser gain media

DOUGLAS HOBBS,[1,*] BRUCE MACLEOD,[1] ERNEST SABATINO,[1] SERGEY MIROV,[2] DMITRI MARTYSHKIN,[2] MICHAEL MIROV,[2] GEORGIY TSOI,[2] SEAN MCDANIEL,[3] AND GARY COOK[3]

[1]*TelAztec LLC, 15 A Street, Burlington, MA 01803, USA*
[2]*IPG Photonics Corporation, 1500 First Avenue North, Birmingham, AL 35203, USA*
[3]*U.S. Air Force Research Laboratory, 2241 Avionics Circle, Wright-Patterson AFB, OH 45433, USA*
[*]*dshobbs@telaztec.com*

Abstract: An expanded study has been completed of the pulsed and continuous wave (CW) laser induced damage threshold (LiDT) of surface relief anti-reflection (AR) microstructures (ARMs) etched in zinc selenide (ZnSe) crystals and chromium-ion-doped (Cr:ZnSe) laser gain media. In multiple-sample per variant testing at wavelengths of 2095 and 2940nm, the pulsed laser damage resistance of ARMs textured ZnSe crystals was found to be equivalent to untreated, as-polished crystals, with an LiDT as much as 5 times that of thin-film AR coated ZnSe crystals. Similar results were found for Cr:ZnSe crystals tested at 2940nm, but mixed results were found for pulse testing at 2095nm. In accumulated power CW damage testing at a wavelength of 1908nm, neither untreated nor ARMs treated ZnSe crystals could be damaged after long duration exposures at a maximum system intensity of 28.6 MW/cm^2, a value many times higher than typically found with thin-film AR coated ZnSe. For Cr:ZnSe gain media, the CW LiDT was observed to be dependent on the focused beam size at the sample surface, with thresholds for untreated and ARMs-treated Cr:ZnSe being nearly equivalent, ranging from 0.6 MW/cm^2 for the largest spot size, to 2.1 MW/cm^2 for a spot area 4 times smaller. An operational laser test was performed where an ARMs textured Cr:ZnSe crystal operated with higher slope efficiency and 1.5 times the output of a thin-film AR coated crystal in an identical resonator configuration.

OCIS codes: (310.1210) Antireflection coatings; (310.6628) Subwavelength structures; (140.3330) Laser damage; (160.6990) Transition-metal-doped materials. (140.3580) Lasers, solid-state; (220.4241) Nanostructure fabrication.

References and links

1. I. Moskalev, S. Mirov, M. Mirov, S. Vasilyev, V. Smolski, A. Zakrevskiy, and V. Gapontsev, "140 W Cr:ZnSe laser system," Opt. Express **24**(18), 21090–21104 (2016).
2. S. B. Mirov, V. V. Fedorov, D. V. Martyshkin, I. S. Moskalev, M. Mirov, and S. Vasilyev, "Progress in Mid-IR Lasers Based on Cr and Fe-Doped II–VI Chalcogenides," IEEE J. Sel. Top. Quantum Electron. **21**(1), 292–310 (2015).
3. H. Krol, C. Grezes-Besset, L. Gallais, J. Natoli, and M. Commandre, "Study of laser-induced damage at 2 microns on coated and uncoated ZnSe substrates," Proc. SPIE **6403**, 640316 (2006).
4. S. McDaniel, D. S. Hobbs, B. D. MacLeod, E. Sabatino, P. A. Berry, K. L. Schepler, W. Mitchell, and G. Cook, "Cr:ZnSe laser incorporating anti-reflection microstructures exhibiting low-loss, damage-resistant lasing at near quantum limit efficiency," Opt. Mater. Express **4**(11), 2225–2230 (2014).
5. D. S. Hobbs, B. D. MacLeod, E. Sabatino III, S. B. Mirov, and D. V. Martyshkin, "Laser damage resistant anti-reflection microstructures for mid-infrared metal-ion doped ZnSe gain media," Proc. SPIE **8530**, 85300P (2012).
6. D. S. Hobbs and B. D. MacLeod, "Design, Fabrication and Measured Performance of Anti-Reflecting Surface Textures in Infrared Transmitting Materials," Proc. SPIE **5786**, 349 (2005).
7. D. H. Raguin and G. M. Morris, "Antireflection structured surfaces for the infrared spectral region," Appl. Opt. **32**(7), 1154–1167 (1993).
8. F. Reversat, T. Berthou, S. Tisserand, L. Dupuy, S. Gautier, P. Muys, D. Delbeke, D. Grojo, M. Laraichi, and P. Delaporte, "Development of diffractive antireflection structures on ZnSe for high power CO2 laser applications," Proc. SPIE **6992**, 699201 (2008).

#296086 https://doi.org/10.1364/OME.7.003377
Journal © 2017 Received 16 May 2017; revised 17 Jul 2017; accepted 16 Aug 2017; published 25 Aug 2017

Optical Materials EXPRESS

9. D. S. Hobbs, B. D. MacLeod, E. Sabatino III, J. A. Britten, and C. J. Stolz, "Contamination resistant antireflection nano-textures in fused silica for laser optics," Proc. SPIE **8885**, 88850J (2013).
10. B. D. MacLeod, D. S. Hobbs, and E. Sabatino III, "Moldable AR microstructures for improved laser transmission and damage resistance in CIRCM fiber optic beam delivery systems," Proc. SPIE **8016**, 80160Q (2011).
11. L. E. Busse, C. Florea, B. Shaw, V. Nguyen, J. S. Sanghera, I. Aggarwal, and F. Kung, "Antireflective surface structures on IR fibers for high power transmission," in *Advanced Solid-State Lasers Congress*, G. Huber and P. Moulton, eds. OSA Technical Digest (online) (Optical Society of America, 2013), paper AM2A.5.

1. Introduction

Progress toward higher power, widely tunable solid-state lasers [1,2] operating over middle-infrared (mid-IR) wavelengths in the 2-5μm range, has been slowed by the inconsistent performance, limited choice of materials, and poor reliability of thin-film anti-reflection (AR) coatings (TFARC) [3]. AR coatings for transition-metal-ion doped II-VI laser gain media such as chromium zinc selenide (Cr:ZnSe) are particularly difficult to deposit due to the material low temperature requirements and the significant water absorption sensitivity, factors tending to yield coatings with low laser damage resistance [4]. A promising approach for removing these limitations is to replace TFARCs with an array of nanometer scale surface relief microstructures etched directly into the polished Cr:ZnSe crystal facets [5]. AR microstructures (ARMs) provide a robust, single material solution exhibiting low-loss, wide angular acceptance, low polarization sensitivity, broad spectral transmission gain, and no susceptibility to water absorption [4–8]. ARMs textures in many optical materials including ZnSe and Cr:ZnSe have been demonstrated with a laser-induced damage threshold (LiDT) that can match the level of a well-polished surface; a survivability many times higher than an equivalent performance broad-band TFARC [9–11].

In a previous study [5], the pulsed LiDT of ARMs textures in ZnSe and Cr:ZnSe was evaluated at a wavelength of 2095nm and found to be comparable to well polished material with no AR treatment. This level was expected to be many times higher than that achievable with thin-film AR coatings. Similarly, the CW LiDT of ARMs textures in Cr:ZnSe showed a damage resistance up to the 0.5 MW/cm^2 level at a wavelength of 1940nm. In this expanded study, the pulsed and CW LiDT of ARMs textures in ZnSe and Cr:ZnSe was directly compared with the LiDT of broad-band thin-film AR coated ZnSe and Cr:ZnSe at three laser wavelengths in the mid-IR.

2. ARMs textures

A microstructure array consisting of cone-like protrusions creates a graded refractive index that allows light to propagate through the crystal facet with minimal losses due to reflection, diffraction or scattering. Referred to as a "Motheye" texture in the literature [6,7], scanning electron microscope images of a Motheye-type hexagonal grid cone array etched in the surface of a ZnSe crystal, is shown in Fig. 1. The grid spacing of the cones in the array is set at 750 nanometer (nm), small enough to avoid losses due to diffraction when operated at wavelengths from 1900 to 3500nm, and the depth of the texture is greater than 1000nm to provide broad-band performance. Motheye arrays are fabricated in ZnSe using a two stage process consisting of the creation of a sacrificial mask layer using interference lithography, followed by reactive ion etching with a unique gas chemistry to avoid defects that are the pre-cursors of laser damage at the grain boundaries of poly-crystalline ZnSe [5,8].

ARMs textures can also be realized as cone-like features with a random distribution of feature height, depth, and spacing. These "Random" AR (RAR) textures have a uniform packing density that avoids losses due to scattering over the desired wavelength band. RAR textures etched in fused silica optics have been extensively demonstrated with ultra-low reflectance over wide bandwidths and with a pulsed and CW laser damage resistance far exceeding TFARCs. Because RAR textures are produced with a single stage RIE process, the

Optical Materials EXPRESS

pattern origination costs associated with Motheye ARMs textures are avoided, and optics can be treated at costs competitive with the highest performing TFARCs. One issue with RAR texture fabrication is that a unique RIE recipe must be developed for each different material. Recent progress has been made in developing an RAR recipe for ZnSe and ZnS. Figure 2 shows an RAR texture defined in the surface of a ZnSe window where the average feature size is on the order of 100nm, the average depth is about 700nm, and the packing density is at least two times tighter than the typical Motheye array spacing shown in Fig. 1 (note the magnification change).

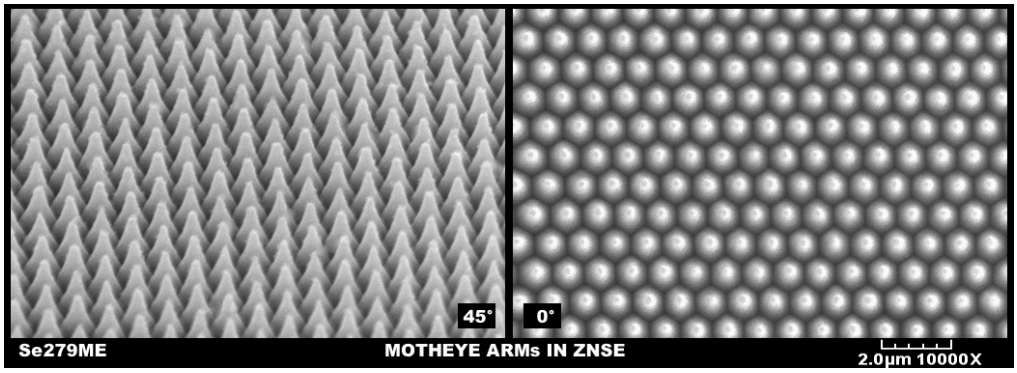

Fig. 1. Elevation (left) and overhead (right) SEM images of a Motheye ARMs texture in ZnSe.

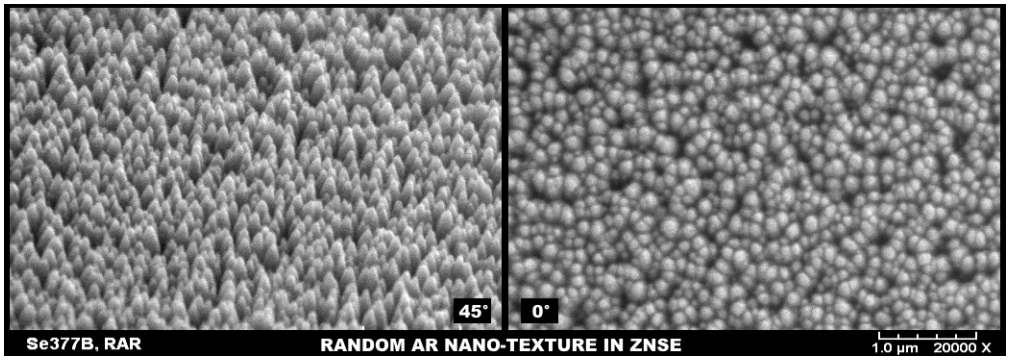

Fig. 2. Elevation (left) and overhead (right) SEM images of a RAR nano-texture in ZnSe.

3. Experimental procedure and results

Polycrystalline ZnSe and multi-spectral ZnS plane parallel round windows were purchased from II-VI Incorporated. Each window, or crystal, was 15mm in diameter, 3.6mm thick, with a commercial grade inspection polish. Several crystals were submitted to IPG Photonics for chromium ion (Cr^{2+}) diffusion to a concentration of $6x10^{18}$ ions per cubic centimeter (cm). A small subset of the chromium doped ZnSe crystals were processed further by IPG to effectively "bleach," or remove the absorption of the chromium ions near the surface to a depth of approximately 0.25mm. The bleaching process is expected to yield significantly higher LiDT values for Cr^{2+} doped laser gain media.

To evaluate the effect of surface quality on LiDT, most of the crystals were ground and polished to a 40/20 scratch/dig specification referred to below as polish level B, while some were polished to a higher level of 20/10 scratch/dig specification referred to as polish level A. Other un-doped windows were maintained in their as-received, uncontrolled inspection polish condition referred to as polish level C.

Optical Materials EXPRESS

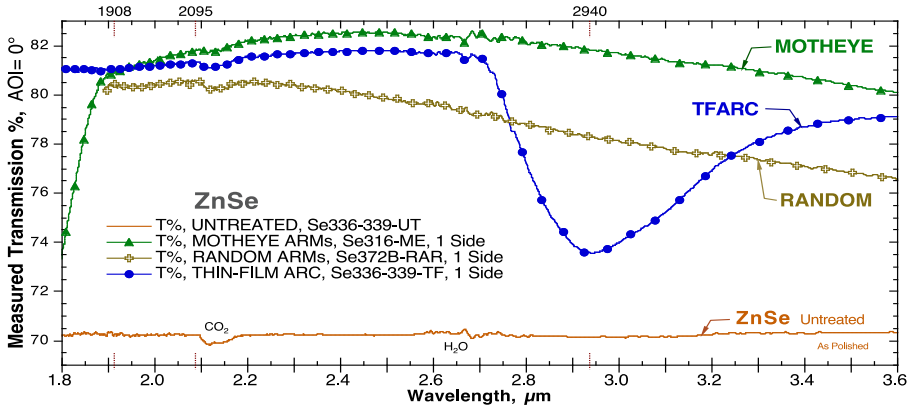

Fig. 3. Measured transmission of untreated, ARMs-treated, and thin-film AR coated ZnSe.

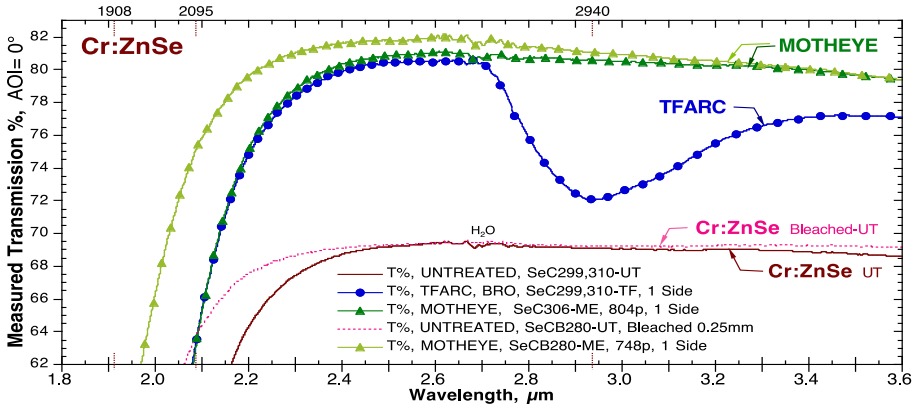

Fig. 4. Measured transmission of untreated, ARMs-treated, and thin-film AR coated Cr:ZnSe.

A matrix of crystal variants were prepared for pulsed and CW laser damage testing at three wavelengths, 2095nm, 2940nm, and 1908nm. Variants included ZnSe (Se), Cr:ZnSe (SeC), bleached Cr:ZnSe (SeCB), and ZnS (CT) materials with polish levels A, B, or C as described above. AR treatments included untreated (UT) crystals with no AR, both Motheye and Random (RAR) ARMs textured crystals, and thin-film AR coated (TFARC) crystals. Figures 3 and 4 compare the measured spectral transmission over the wavelength range of 1800nm to 3600nm for typical Se, SeC, and SeCB crystals included in the matrix of variants. Of note is the significant broad-band absorption centered near 3000nm for the thin-film AR coated crystals that is due to the presence of water in the coating material layers (blue curve with solid circle markers). The inclusion of water in thin-film AR coatings is a common problem that is difficult to overcome, and is one of the issues that drive the development of water adsorption resistant ARMs technology. The Motheye, RAR, and TFARC samples shown were treated one surface only, making the maximum transmission possible at 82.5% for these ZnSe and Cr:ZnSe crystals over this spectral band.

3.1 Pulsed laser damage testing at 2095nm

Twelve ZnSe crystals and seven Cr:ZnSe crystals were submitted to SPICA Technologies for pulsed LiDT testing following the s-on-1 standard in ISO 11254, with s being the number of pulses delivered at a fixed fluence level to a single site on a test sample surface. The destructive test employed a Ho:YAG laser emitting a well collimated, Gaussian intensity profile, TEM_{00}

Optical Materials EXPRESS

circular beam at a wavelength of 2095nm that is focused at normal incidence onto the sample surface with a controlled spot size of 230µm, or 0.23mm ($1/e^2$). One hundred locations mapped on a 0.8mm square grid within the central 10mm diameter circular area on each crystal, were exposed to one of as many as 12 fluence levels. Up to 200 pulses were delivered at each exposure site, each pulse having a 60 nano-second (ns) duration (FWHM), and repeating at a 100Hz rate. Other beam parameters were multiple longitudinal modes, and a random polarization state. SPICA determines the damage threshold using the "Least Fluence Failure" method, meaning the fluence level immediately preceding the level that causes permanent surface damage. Observation of damage is accomplished through microscopic imaging of the exposure site using a Nomarski configured microscope at a magnification of 150 times normal size.

The data for damage frequency as a function of exposure fluence can often be fit to a linear function. Figure 5 shows the raw data and linear fit to the data for three of the Cr:ZnSe crystals tested. The Least Fluence Failure threshold is found at 4.0, 3.5, and 3.0J/cm^2 for the untreated (red open crosses), Motheye-textured (solid green triangles), and thin-film AR coated (solid blue squares) crystals respectively, whereas the best fit linear thresholds are as listed by the curve labels at 4.1, 3.3, and 3.0J/cm^2. Table 1 below lists the threshold data for all ZnSe samples tested as well as the quality of the linear fits.

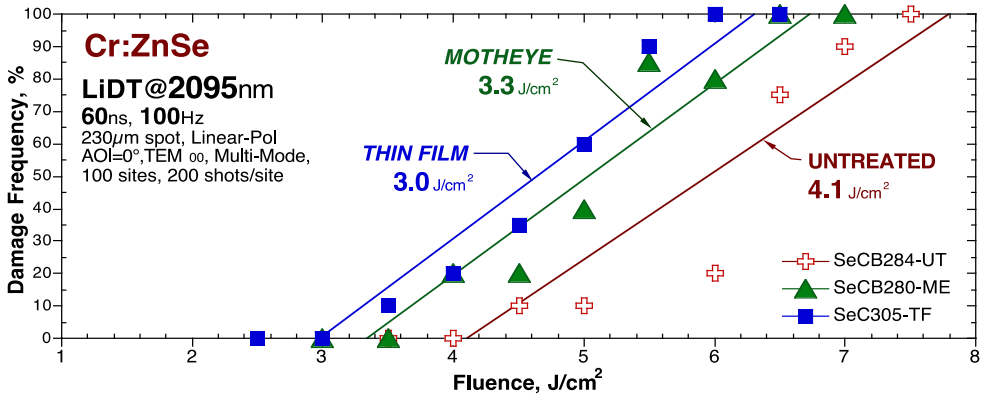

Fig. 5. Damage frequency for untreated, Motheye-textured, and thin-film AR coated Cr:ZnSe as a function of exposure fluence (2095nm wavelength, 60ns pulse width, 100Hz rep rate).

Table 1. ZnSe LiDT, J/cm2, @ 2095nm, 60ns, 100Hz, 0.23mm spot area.

MAT	Se	Se	Se	Se	Se	Se	Se	Se	Se	Se	Se	Se
ID	307	327	308	309	311	272	257	265	316	318	337	336
VAR	**UT**	**UT**	**UT**	**UT**	**UT**	**ME**	**ME**	**ME**	**ME**	**ME**	**TF**	**TF**
LiDT	**3.0**	**5.0**	**7.0**	**5.0**	**4.0**	**3.5**	**5.0**	**6.0**	**5.5**	**3.0**	**3.5**	**4.0**
FIT	2.6	4.7	6.2	5.3	3.2	3.3	5.6	6.2	4.7	2.7	3.9	3.4
FIT R	.97	**.99**	**.99**	**.93**	.98	**.93**	**.90**	**.92**	**.93**	.97	.97	.98

Despite continual advancement in AR treatment processing and damage testing procedures, the data from Fig. 5 and Table 1 is somewhat scattered indicating an undesirable influence of factors that are difficult to control such as sample heating, polish level and surface cleaning. Visualizing the data set as a whole using the bar chart of Fig. 6, an average of the LiDT values for each variant supports the conclusion that Motheye textured surfaces have a damage resistance that is close to that of the polished surfaces, and that this resistance is about 25% higher than the damage resistance of thin-film AR coated surfaces. Note that for these tests, the expected increase in damage resistance with better surface quality was not observed (polish level A having fewer scratches and digs than polish levels B and C as indicated in the figure).

Optical Materials EXPRESS

In fact the A polish level for the untreated and Motheye textured Cr:ZnSe samples may have had the opposite effect yielding a reduced damage resistance. Better surface quality is obtained with longer polishing times which could have produced more sub-surface damage than shorter polishing time – one possibility to explain the results.

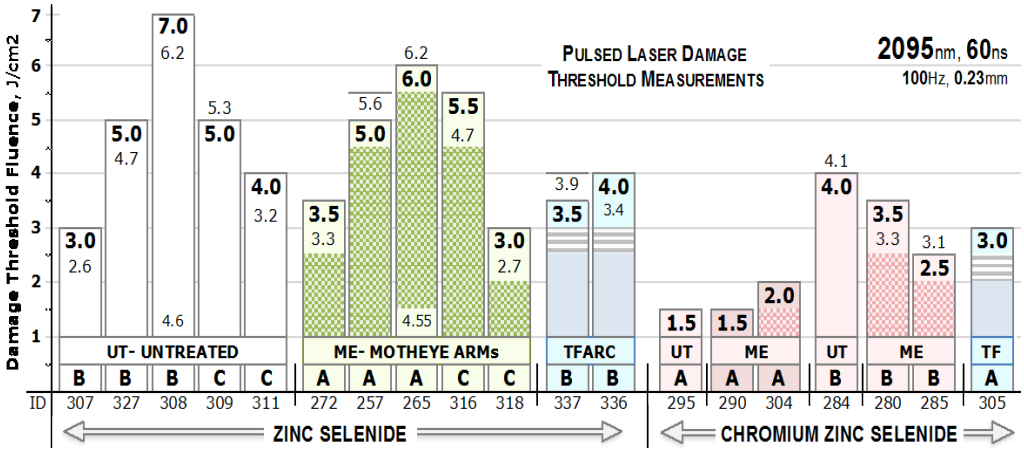

Fig. 6. Bar chart comparing the pulsed LiDT data collected by SPICA for UT, ME, and TF AR coated ZnSe and Cr:ZnSe crystals (2095nm, a pulse duration of 60ns, and a 0.23mm spot area).

3.2 Pulsed laser damage testing at 2940nm

At longer operational wavelengths for Cr:ZnSe laser systems, particularly higher power tunable systems, residual water incorporated within thin-film coatings produces undesirable absorption in the 2700-3200nm range that severely limits laser function. To further illustrate this limitation and the benefits of ARMs technology, a set of 14 ZnSe and 6 Cr:ZnSe crystals were submitted to Quantel USA for pulsed LiDT testing at a wavelength of 2940nm. Quantel conducted 200-on-1 ISO 11254 standard pulsed testing using their Er:YAG laser configured for an 100ns pulse width, 4Hz rep rate, and 0.41mm spot size. The results of these tests are unambiguous showing damage thresholds for Motheye-textured and UT crystals as nearly equivalent at a level between 2 and 5 times higher than the TFARC crystals. The result is most dramatic for the un-doped ZnSe crystals where multiple Motheye and RAR textured crystals show a damage resistance 5 times higher than the two TFARC crystals tested.

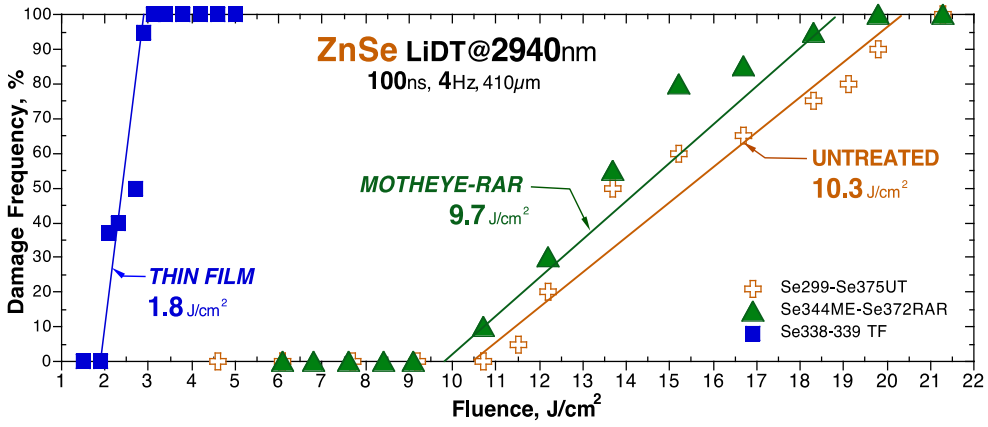

Fig. 7. Damage frequency for untreated, Motheye-textured, and thin-film AR coated ZnSe crystals as a function of exposure fluence (2940nm wavelength, 100ns pulse width, 4Hz).

Optical Materials EXPRESS

Similar to Fig. 5 above, Fig. 7 is a plot of the damage frequency versus the exposure fluence level where an average of two samples for each variant (UT, ME/RAR, TFARC) is shown along with a linear fit. Figure 8 shows a bar chart comparing all the threshold data collected with like variants grouped together. As with the 2095nm testing, these 2940nm test results show no correlation between damage resistance and polish level.

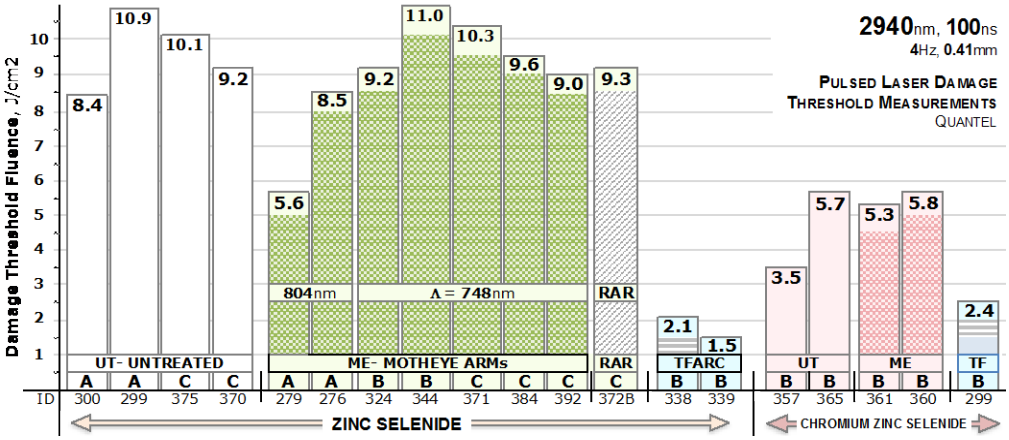

Fig. 8. Pulsed LiDT data for untreated (UT), Motheye (ME) and Random AR-textured (RAR), and thin-film AR coated (TF) ZnSe and Cr:ZnSe laser crystals at a wavelength of 2940nm.

3.3 CW laser damage testing at 1908nm

The CW laser damage resistance of ZnSe and Cr:ZnSe laser crystals was investigated using an apparatus and method established by IPG Photonics that is similar to that described in our earlier 2012 publication [5]. For this work, the number of exposure sites per sample was increased for a more statistically relevant determination of the damage threshold. As many as 60 sites for one sample were exposed to accumulated power levels below and above the average intensity value that caused damage, a value specific to each AR variant. Sites were mapped to a square grid with 1mm spacing where only grid points within a 12mm diameter circular area centered on each 15mm diameter crystal were exposed.

The 1908nm wavelength emission from an IPG Photonics model TLR-100-WC-Y12 100W thulium fiber laser was chosen over the 1940nm source used in the 2012 testing [5] due to the shorter wavelength being better aligned with the peak Cr^{2+} absorption combined with larger output power and high quality spatial mode. Figure 9 shows the experimental setup. The randomly polarized diverging beam from the fiber laser is directed through collimating lens L1 to establish a beam diameter of approximately 3mm ($1/e^2$). A portion of the beam is then reflected by an uncoated wedge optic W onto detector D1 (Ophir Thermopile model Nova II 30A-BB-18) that serves as a monitor for the incident power level. (A beam dump captures the displaced second surface reflection from the wedge.) The main portion of the beam is then focused onto the surface of the laser crystal under test by a plano-convex lens L2 to a calibrated spot size and location. The spot diameter was incrementally reduced from 80 micrometer (μm) to 40μm, and then 20μm using L2 lenses with 100, 50, and 25mm focal lengths giving maximum intensity levels of 1.7, 7.5, and 28.6 million watts per square cm (MW/cm^2) respectively. After passing through the crystal, the beam is captured by detector D2 (Ophir model Vega FL250A-V1) that monitors the transmitted power level and controls shutter S to rapidly close upon initiation of damage.

Testing begins by ramping the laser power to its maximum output with no sample in the system to establish the calibration of detectors D1 and D2, the incident and transmitted powers respectively. Next each crystal is attached to a water-cooled metal holder that provides adequate

Optical Materials EXPRESS

heat removal during the testing. The holder was fixed on a computer controlled XY translation table that positions the crystal at the chosen exposure point in the grid described above. An exposure starts at a low power level typically below 10W that is held for 10 seconds and then incremented in 2% steps, also with a 10sec dwell time, increasing until damage occurs as indicated by a rapid drop in transmitted power, or until the highest power level planned for that site is reached in which case the power is held for a total exposure duration of 15 minutes (900sec).

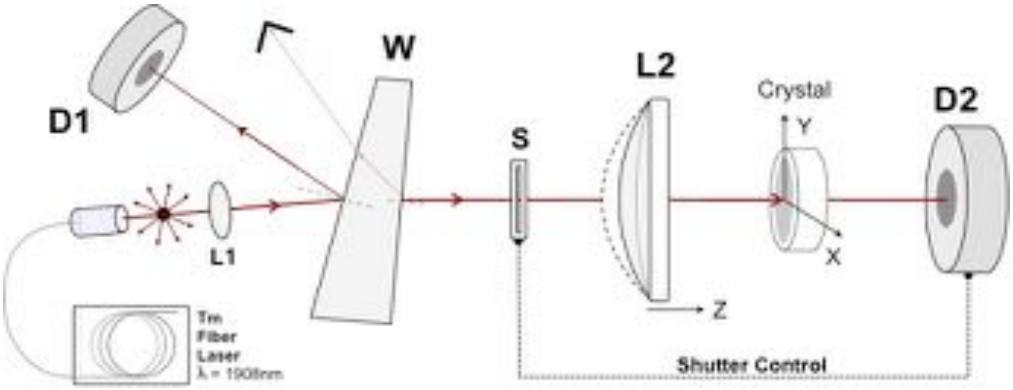

Fig. 9. Experimental setup for accumulated power CW laser damage testing at 1908nm.

Figure 10 charts the calibrated incident (blue curves) and transmitted (green, amber, and red curves) power data recorded by detectors D1 and D2 over the exposure time for one site on four different crystals, two ZnSe crystals shown on the left, and two Cr:ZnSe crystals shown on the right. Diagrams inset to each chart show the specific shot location on each crystal surface. Referring to the left side chart for the untreated (amber, Se340-UT) and the ME-textured (green, Se258-ME) ZnSe crystals, it can be seen that the transmitted power for both samples tracks the incident power for the entire 15-minute exposure indicating no damage. Note that the transmitted power for the untreated ZnSe after reaching maximum incident power of 90W is about 63W, which is consistent with the expected 70% transmission for 1908nm light through a ZnSe window as shown in Fig. 3. The single surface ME-textured window shows about 80% transmission, also in line with the Fig. 3 data. None of the five ZnSe crystals, 2 ME-textured and 3 untreated could be damaged at maximum laser power with any of the three focusing lenses indicating a damage threshold no less than 28.6MW/cm^2, a level far exceeding the expected damage threshold for any type of thin-film AR coating on ZnSe. Note that two untreated (no AR) multispectral ZnS windows also could not be damaged in this system after multiple exposures up to the maximum intensity of 28.6MW/cm^2.

Due to heating from absorption by the Cr^{2+} ions, Cr:ZnSe crystals damage at much lower exposure intensity as indicated by the data shown in the chart on the right side of Fig. 10. Here the dashed green and dashed light blue curves show the transmitted and incident power for a Motheye-textured Cr:ZnSe crystal (SeC312-ME), while the solid red and blue curves show the transmitted and incident power for an untreated (no AR, as-polished) Cr:ZnSe crystal (SeC301-UT). Both crystals survive for more than 120 seconds as the incident power is stepped from 7.5W to 30W after which damage occurs during the transition to 32W incident power for the Motheye-textured crystal, and during the transition from 32W to 34W for the untreated crystal. For the 80µm spot area (100mm focal length lens L2), the damage threshold intensity is about 0.65MW/cm^2.

With the ability to rapidly shutter the incident beam at the moment that transmitted power drops, damage to the crystal surfaces outside the immediate area of the exposure was kept to a minimum. Therefore each crystal could be exposed at many other locations and for Motheye-textured Cr:ZnSe crystal SeC312-ME and untreated crystal SeC301-UT, 32 and 47 additional

Optical Materials EXPRESS

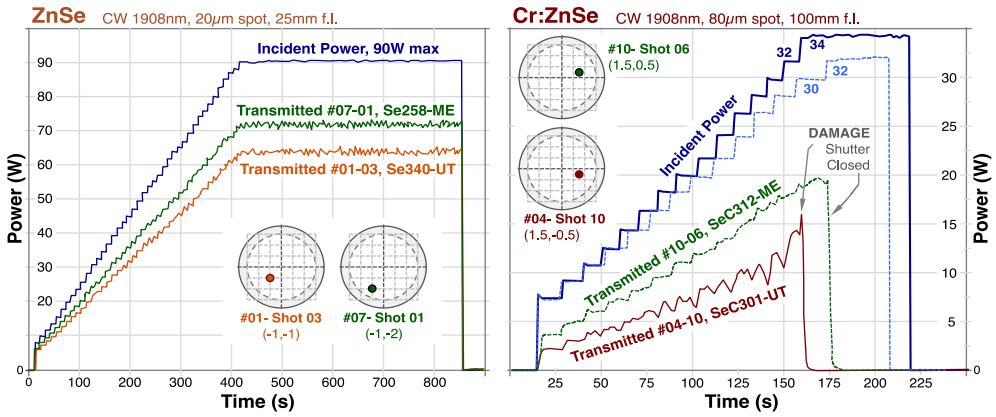

Fig. 10. Measured incident and transmitted power over time for UT (no AR) and Motheye-textured ZnSe (left) and Cr:ZnSe (right) . Dashed curves are used for the Motheye-textured Cr:ZnSe data. Inset graphics show the exposure location on the surface of individual samples.

locations (respectively) were exposed to a range of power levels to yield more statistically relevant information regarding CW damage resistance. Figure 11 plots this damage frequency data as a function of exposure intensity where the solid light green triangles mark the Motheye-textured crystal data and open red crosses mark the untreated crystal data. Solid lines are also plotted to show a linear fit to the damage data. This analysis indicates a damage threshold of 0.6 MW/cm^2 for both the as-polished and Motheye-textured crystals, a value consistent with the 0.5 MW/cm^2 threshold found for 1940nm wavelength exposures in our earlier work [5]. Damage frequency data for two additional crystals exposed with higher intensity using a focused spot area of 40μm (50mm focal length lens L2), are also included in Fig. 11. A damage threshold of 2.1MW/cm^2 is indicated by a linear fit to each data set for both the as-polished crystals (#SeC398-UT, open dark red cross markers), and the Motheye-textured crystals (#SeC383-ME, dark green triangle markers). This approximately 3.5 times higher threshold found with the 40μm spot diameter is presumably due to the exposure area being reduced to one quarter that of the 80μm spot area exposures, and therefore being less likely to encounter surface defects or surface contaminants that are the precursors of damage.

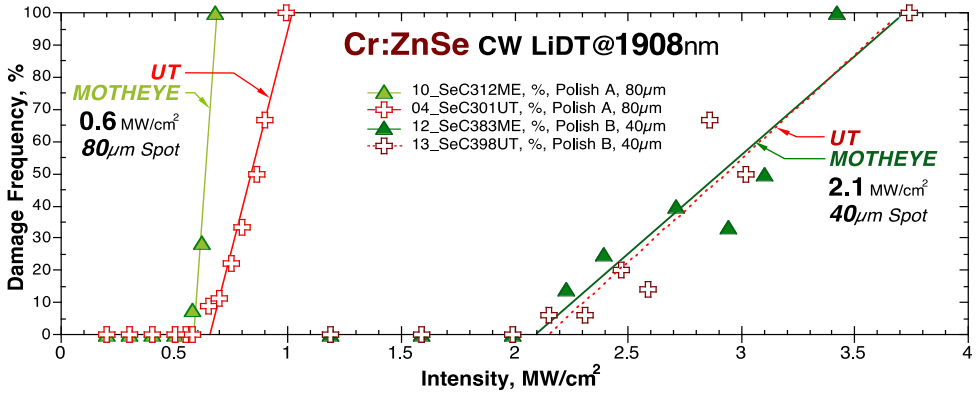

Fig. 11. Damage frequency as a function of exposure intensity for untreated (open cross markers) and Motheye-textured (solid triangle markers) Cr:ZnSe crystals using focused beam diameters of 80μm (left) and 40μm (right).

For comparison, IPG exposed one of their Cr:ZnSe laser crystals with a thin-film AR coating (deposited by Rocky Mountain Instrument of Colorado) using the Fig. 9 system configured with a 25mm focal length lens L2 for a 20μm exposure spot diameter on the crystal surface. Damage occurred at an intensity of 2.8MW/cm^2 for this 20μm spot size, a threshold

Optical Materials EXPRESS

that would scale to 0.80 and 0.23MW/cm^2 for larger area exposures with the 40µm and 80µm spot diameters respectively. This damage threshold is about three times lower than that found with the untreated and Motheye-textured Cr:ZnSe crystals, and the result is consistent with IPG's expectations and experience with thin-film AR coatings for Cr:ZnSe deposited by a variety of vendors and techniques.

As indicated by the no less than an order of magnitude higher LiDT of un-doped ZnSe compared to Cr^{2+}doped ZnSe, laser damage is strongly linked to absorption in or near the surface of laser crystals. A Cr:ZnSe laser crystal design incorporating un-doped or bleached exit and entrance facets ("end-caps"), as well as Motheye AR nano-textures etched in the facets, likely offers the greatest level of damage resistance and long-term reliability for power scaled systems. A Cr:ZnSe disc was bleached by IPG to remove the chromium ion absorption from all surfaces to a depth of approximately 0.5mm, and then Motheye AR nano-textures were fabricated in one surface. This bleached crystal (#SeCB281ME) was subjected to extensive damage testing within the Fig. 9 system where over 60 sites were exposed to increasing intensities. Initially 36 locations were exposed using the 80µm spot size with no damage found up to the maximum intensity of 1.7 MW/cm^2, a level at least 3 times higher than the un-bleached and Motheye-textured Cr:ZnSe crystals exposed to the 80µm spot size (Fig. 11). An additional six new locations were then exposed to the maximum intensity attainable with the 40µm spot size, 7.5MW/cm^2, and again no damage was observed at any site for the entire 15min duration exposures. Finally the spot size was decreased to 20µm and 25 new locations were exposed. In this configuration damage was observed at 9 locations for various intensity levels where a linear fit to the damage frequency data (as in Fig. 11) indicates a damage threshold above 11MW/cm^2, effectively demonstrating the benefits of eliminating surface absorption through the combination of Motheye textures with chromium ion bleaching.

3.4 Laser system testing

The Air Force Research Laboratory (AFRL) at Wright Patterson Air Force Base conducted an operational laser system test similar to that reported previously [4], with this test intended to push the limits of the resonator to the point of damage at the input facets of the Cr:ZnSe gain media. Measurement of the resonator slope efficiency were made to compare the performance of Motheye textured crystals to thin film AR coated crystals, where the incident pump power was incremented beyond the output saturation and the thermal quenching level, and finally to catastrophic failure.

The experimental setup is shown in Fig. 12. The 1908nm wavelength emission from a thulium fiber laser pump (a 120W IPG Photonics model TLR-120-WC-Y12) was focused into the resonant cavity using a 10 cm focal length lens, L1, to a spot diameter of 132µm (1/e^2) at the face of the crystal. Dichroic mirror M1 has a 50mm radius of curvature (ROC) and was AR coated on the input face to pass the 1908nm pump, with a multi-layer dielectric coating stack on the cavity face that also passes 1908nm light and serves as a high reflector (HR) for the laser resonator wavelength range from 2000 to 3000nm. A second dichroic mirror M2 with a 100mm ROC and the same AR/HR function as M1, is used to fold the resonator cavity and shape the intra-cavity mode to efficiently fill the Cr:ZnSe gain media to a fundamental mode size of approximately 120µm. Mirror M3 was a 70% reflective output coupler for the 2300-3000nm wavelength range. Incident pump power was measured at the laser source, and laser output power was recorded by detector D1. Active cooling of the Cr:ZnSe crystals was accomplished using a flowing water jacket mounting system. As with the previously described damage testing, the Cr:ZnSe discs were 3.6mm thick with a diameter of 15mm and a Cr^{2+} ion concentration of 6x10^{18} ions/cm^3. One Motheye-textured crystal and one thin-film AR coated (also by Blue Ridge Optics) crystal were evaluated.

The resonator configuration shown in Fig. 12 realizes a larger incident spot size (132µm) compared to the previous work (65µm) [4] due to the use of a new fiber laser pump with improved spatial mode at higher output power. Results from the earlier work with the smaller

Optical Materials EXPRESS

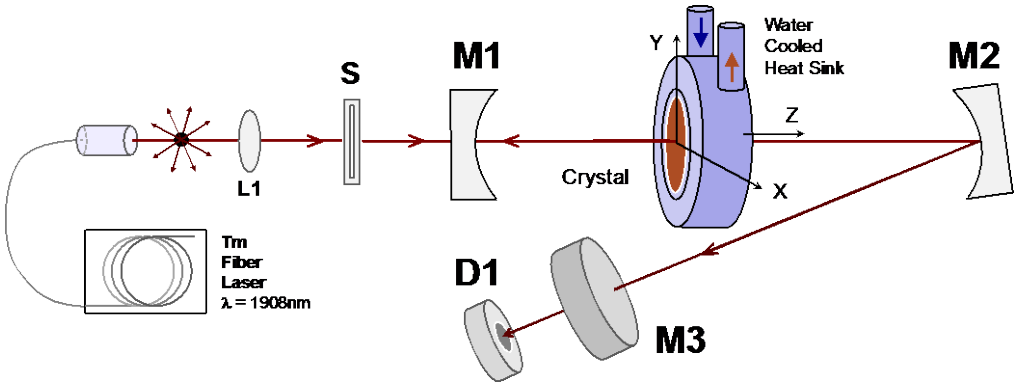

Fig. 12. Diagram of the Cr:ZnSe laser configuration used for the operational testing.

cavity beam and 70% out-coupler, showed slope efficiencies for Motheye-textured and thin-film AR coated crystals of 68% and 52% respectively. In this work, with the larger beam and same 70% out-coupler, the slope efficiency of the Motheye-textured crystal was 59%, while the thin-film AR coated crystal was considerably lower at 40%. Figure 13 plots the resonator output power as a function of incident pump power for the two resonators formed with the Motheye-textured crystal (solid green triangles), and thin-film AR coated crystal (solid blue squares). Both resonators exhibited the onset of thermal quenching at approximately 10W of absorbed power. However, at the point of thermal quenching, the Motheye-textured crystal resonator produced approximately 50% more output than the thin-film AR coated crystal. Motheye-textured crystals are likely to maintain this benefit for long operational times compared to thin-film AR coated crystals where water absorption in the film layers over time further increases cavity losses.

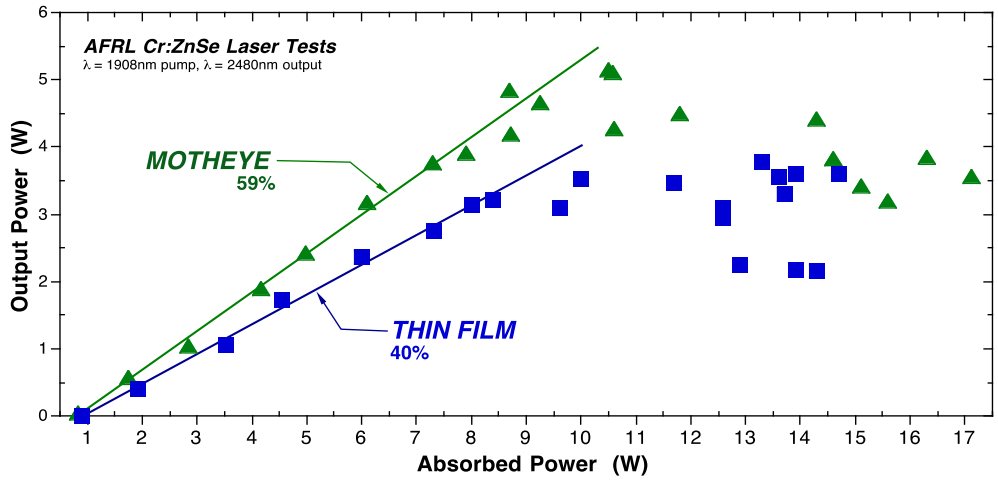

Fig. 13. Slope efficiencies of Motheye textured and TFARC crystals in identical resonators.

The pump power was then further increased until damage occurred on the input facets of the crystals. It should be noted that above 10W of absorbed power, thermal processes within the crystals caused the output of the laser to become erratic. As pump power is further increased closer to the damage threshold of the crystal surfaces, the Cr:ZnSe laser output power fell to less than 100mW due to the decrease in the excited state lifetime of the material, and cavity instabilities related to thermal lensing. The Motheye sample damaged at 91W of incident power, which corresponds to an intensity of 0.66MW/cm^2. The TFARC sample damaged at an incident power of 79W, an intensity of 0.58MW/cm^2.

Optical Materials EXPRESS

Post-exposure inspection of the damage sites shows dramatic differences in the nature of the sample failure, as shown in Fig. 14. The damage on the Motheye-textured crystal exhibited bulk melting and splattering due to localized heating of the material, without evidence of crystal fracture. The thin-film AR coated crystal damage comprised catastrophic fracture of the laser crystal and coating delamination, presumably due to the large stress induced by the coating arising from surface absorption and differential thermal expansion.

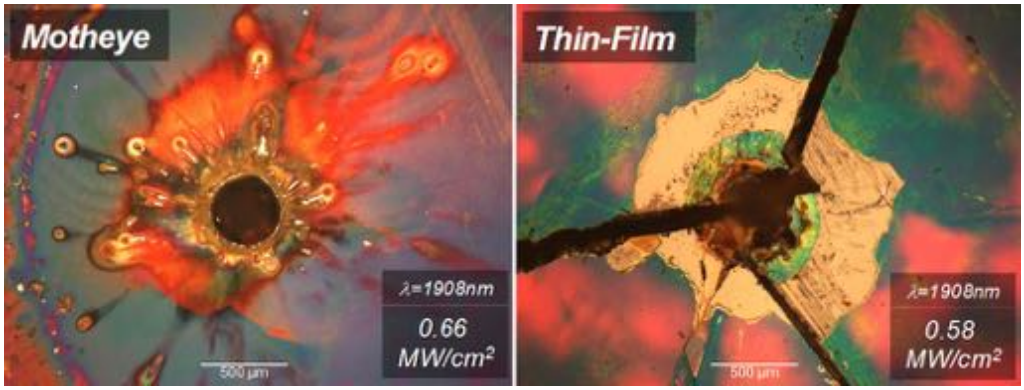

Fig. 14. CW laser damage on Motheye textured (left) and thin film AR coated (right) crystals.

4. Conclusion

Motheye type AR nano-textures were fabricated in ZnSe and Cr:ZnSe crystals demonstrating low reflection loss over a 1500nm wide spectral range in the mid-IR. Through a series of standardized CW and pulsed LiDT testing at three laser wavelengths, the damage resistance of AR nano-textured crystal facets was shown to be equivalent to a well polished surface, a level in some cases many times higher than that found for thin-film AR coated crystal facets. The increased power handling is due in part to the elimination of surface absorption inherent with AR nano-textured interfaces, and in part to the elimination of water band absorption that is prevalent in most thin-film AR coating materials and deposition processes. By removing surface absorption, surface heating that leads to thermal lensing and bulk stresses is minimized which extends the performance, power handling, and lifetime of the laser crystal. A practical demonstration of this benefit was made through operational laser tests conducted by AFRL that showed greater output power and higher damage resistance for Motheye-textured gain media compared to thin-film AR coated gain media. The gains demonstrated by this single wavelength laser test are expected to increase significantly for tunable laser systems operating at longer wavelengths where water absorption currently limits power scaling and reliability.

Funding

Air Force Research Laboratory, Sensors Directorate, Wright-Patterson Air Force Base, through SBIR contract FA8650-12-C-1367. Cleared for public release; case # 88ABW-2017-2336.

Acknowledgments

The authors also thank Mike Thomas and Andrew Griffin of SPICA Technologies for the detailed pulsed LiDT testing at 2095nm, and Jason Yager of Quantel for the detailed pulsed testing at 2940nm.